

Macro- and Microscale Investigation of Selenium Speciation in Blackfoot River, Idaho Sediments

LIBBIE L. ORAM,^{*,†}
DANIEL G. STRAWN,^{†,‡}
MATTHEW A. MARCUS,^{||}
SIRINE C. FAKRA,^{||} AND
GREGORY MÖLLER^{†,§}

Environmental Science Department, Department of Plant, Soils, and Entomological Sciences, and Department of Food Science and Toxicology, P.O. Box 442339, University of Idaho, Moscow, Idaho 83844-2339, and Lawrence Berkeley National Laboratory, Berkeley, California

Received December 21, 2007. Revised manuscript received April 3, 2008. Accepted April 10, 2008.

The transport and bioavailability of selenium in the environment is controlled by its chemical speciation. However, knowledge of the biogeochemistry and speciation of Se in streambed sediment is limited. We investigated the speciation of Se in sediment cores from the Blackfoot River (BFR), Idaho using sequential extractions and synchrotron-based micro-X-ray fluorescence (μ -SXRF). We collected μ -SXRF oxidation state maps of Se in sediments, which had not been done on natural sediment samples. Selective extractions showed that most Se in the sediments is present as either (1) nonextractable Se or (2) base extractable Se. Results from μ -SXRF showed three defined species of Se were present in all four samples: Se(-II,0), Se(IV), and Se(VI). Se(-II,0) was the predominant species in samples from one location, and Se(IV) was the predominant species in samples from a second location. Results from both techniques were consistent, and suggested that the predominant species were Se(-II) species associated with recalcitrant organic matter, and Se(IV) species tightly bound to organic materials. This information can be used to predict the biogeochemical cycling and bioavailability of Se in streambed sediment environments.

Introduction

Phosphorus mining in the U.S. Western Phosphate Resource Area (WPRA) in Idaho and Wyoming has moved selenium (Se) from a relatively stable subsurface setting to the near surface, which is a much more dynamic weathering environment. Selenium occurs naturally in the middle waste shale, a mining byproduct, at concentrations up to 250–300 mg Se kg⁻¹ (1, 2). Recent sequential extraction and X-ray absorption spectroscopic studies have determined that Se in the waste shale exists primarily as reduced Se(-II) or elemental Se species (3, 4). Despite the low solubilities of these reduced Se phases, in oxidizing environments reduced Se reacts to form soluble Se(IV) and Se(VI) oxyanion species,

resulting in offsite transport into the contiguous watershed (Blackfoot River (BFR), Idaho) and ecosystem. In this lotic environment, mine drainage and soil erosion transfer seleniferous leachates and suspended particles from reclaimed soils into nearby surface waters and sediments. By these means, water facilitates exposure of Se to aquatic and terrestrial ecosystems, and Se toxicity has affected wildlife and livestock in the area (5–7).

In natural environments, Se may be found in four different oxidation states (-II, 0, IV, and VI), partitioned into diverse organic and inorganic phases with varying chemical reactivities. Biogeochemical cycling of Se in sediments controls solubility, transport, and bioavailability, but specific processes are not well understood (8, 9). Because of the uncertainties regarding bioavailability and leachability, research on Se speciation and biogeochemistry is necessary to accurately evaluate risks and manage Se hazards in aquatic environments.

A variety of operationally defined sequential extraction techniques have been developed to characterize the speciation, mobility, and bioavailability of Se in soils and sediments (10–13). Sequential extraction techniques are readily available and allow multiple samples to be analyzed and compared. Drawbacks of sequential extractions include failure to address analyte redistribution during extraction, lack of selectivity, and alteration of sample characteristics and/or speciation during fractionation steps (13). Furthermore, heterogeneous sediment systems demonstrate variability in numerous processes at different scales. Thus, it is critical that both macro- and microscale experiments be conducted to fully probe Se speciation in sediments.

Synchrotron-based X-ray absorption spectroscopy (XAS) allows quantitative determination of Se oxidation states in natural samples under environmentally relevant conditions (14). XANES (the near edge region of the XAS spectrum) can be used to differentiate Se species due to a spectral shift in the absorption edge of each species. However, the collection of XANES spectra requires extended exposure of the sample that can cause radiation-induced changes in oxidation states of elements such as Se and As (15–17). Sutton et al. (18) measured the distribution of Se oxidation states in sediments spiked with selenate by deconvoluting synchrotron-based micro-X-ray fluorescence (μ -SXRF) maps collected at monochromatic energies that were optimized for detection of particular Se oxidation states. Pickering et al. (19) used SXRF to probe two chemical species of Se, selenomethionine and selenate, at 100- μ m resolution in spiked plant tissues, and further quantified each species. Energy-dependent μ -SXRF mapping allows for a low detection limit, in situ analysis, the collection of spatially resolved information on chemical speciation at the microscale, and a short acquisition time (a fraction of a second) at each pixel, minimizing radiation damage.

Experiments presented in this paper investigate Se speciation in natural sediment samples using μ -SXRF mapping at 10–20 μ m resolution. Very few studies have mapped native Se in natural samples (i.e., not spiked). The existing national water quality criterion for Se, 5 μ g L⁻¹, is under review, and research has proposed both a lower criterion, 2 μ g L⁻¹ (20, 21), and a sediment-based criterion (22). The research presented herein investigates native Se speciation at water and sediment concentrations relevant to the proposed standards. Microprobe results are compared to those from sequential extraction techniques, and results from both techniques are interpreted to determine Se speciation in upper Blackfoot River sediments.

* Corresponding author phone: 208-885-9239; e-mail: lloram@vandals.uidaho.edu.

[†] Environmental Science Department, University of Idaho.

[‡] Department of Plant, Soils, and Entomological Sciences, University of Idaho.

[§] Department of Food Science and Toxicology, University of Idaho.

^{||} Lawrence Berkeley National Laboratory.

Materials and Methods

Sampling. The upper Blackfoot River (BFR) originates at the confluence of Diamond Creek and Lanes Creek in an open marsh and grassland in the Caribou National Forest, Caribou County, Idaho. Sampling sites were selected from the BFR headwaters to the lower end of the Blackfoot Reservoir. Nine sites were sampled during three sampling events, 9/28/2004, 6/7/2005, and 8/12/2005 (Figure S1 in Supporting Information (SI)). The sites were numbered consecutively from waypoint 01 at the head of the BFR to waypoints 10 and 11 at the delta and discharge of the Blackfoot Reservoir. At each waypoint (WP), sediment cores and water samples were collected and placed on ice for transport to the laboratory (additional details in SI). Water temperature, GPS coordinates, and surface water pH were recorded at each waypoint. Following the sampling event, water samples were stored at 4 °C. Cores were divided into 3 cm sections and stored under argon-purge at -15 °C. The samples are hereafter termed by their waypoint location at depth (e.g., 04A represents sample from WP 04 at 1–3 cm, and 04G represents sample from WP 04 at 19–21 cm).

Total Selenium Analysis. The sediment cores and water samples were submitted to the University of Idaho Analytical Sciences Laboratory (UIASL) for total Se analysis. The UIASL is a certified drinking water laboratory and state-wide reference laboratory that utilizes USEPA validated methods. Additional details are given in SI.

Sequential Extractions. Sequential extractions were done on the surface and bottom segments of the cores from waypoints 01, 04, 09, 10, and 11 from the August 2005 sampling event. Two replicate extractions were done on each sample. The protocol outlined by Kulp and Pratt (10) without the chromium reduction step was used to selectively fractionate Se (details in SI). In short, the protocol uses the following reagents to target distinct, operationally defined Se species: (1) 18 M Ω -cm type I water (soluble Se(VI), Se(IV), and soluble organic Se compounds); (2) 0.1 M phosphate buffer (K₂HPO₄–KH₂PO₄ buffer (P-buffer)) (ligand-exchangeable Se(IV) or Se found in proteins); (3) 0.1 M sodium hydroxide (NaOH) (tightly sorbed Se(IV) and humic and fulvic organo-selenides); (4) 1 M sodium sulfite (Na₂SO₃) (elemental Se); (5) 15% acetic acid (CH₃CO₂H) (Se(VI) substituted into the carbonate matrix); and (6) USEPA 3050 digest (nonextractable metal selenides and organo-Se compounds).

X-ray Spectroscopy. Micro-SXRF mapping was conducted on beamline 10.3.2 at the Advanced Light Source (ALS), Lawrence Berkeley National Laboratory (Berkeley, CA). A monochromatic X-ray beam tunable to energies from 3–17 keV using a Si(111) crystal set was focused on the sample using a Kirkpatrick–Baez (K–B) mirror pair (23). A seven-element germanium detector was then used to measure the sample fluorescence. Gray orthorhombic elemental Se (Se(0) from Aldrich Chemical Co.) was used to calibrate the monochromator to 12658.0 eV at the inflection point.

For μ -SXRF mapping, the beam was focused to 7 μ m \times 7 μ m, with a dwell time of 200 ms per pixel and a step size of 20 μ m \times 20 μ m. Selenium species distribution maps were collected for reduced Se (Se(0) and Se(II-)), Se(IV), and Se(VI) by scanning the regions of interest at three specific energies. To minimize signal interference from the other species when collecting chemical state maps, the beam energy was tuned to an energy near the maximum signal difference between the Se species. The five energies selected for mapping were as follows: 12659.0 eV (E1) to maximize absorption of Se(-II,0), 12663.5 eV (E2) to maximize absorption of Se(IV), 12668.5 eV (E3) to maximize absorption of Se(VI), 12608.0 eV (E0) (50 eV below the Se edge) for background determination and subtraction, and 12778.0 eV (E4) (100 eV above the Se edge) for signal normalization. Differentiation of Se(-II) and Se(0) is not possible in these samples because of signal

overlaps (details in SI). Energy-dependent μ -SXRF maps were collected on samples 04A, 04G, 09A, and 09C (details in SI).

The windowed X-ray fluorescence counts for Ca, Cr, Cu, Fe, K, Mn, Ni, S, Se, Si, Ti, and Zn were collected as the sample was two-dimensionally rastered through the beam. Each energy dependent map was corrected for deadtime and slight sample-position shift between maps using LabVIEW based software developed at ALS beamline 10.3.2. For Se species identification, μ -SXRF maps were deconvoluted for signal overlap according to the method of Sutton et al. (18) (details in SI).

Results and Discussion

Selenium in Water and Sediments. Surface water Se concentrations in the BFR ranged from less than 1 μ g Se L⁻¹ (method detection limit) to 1.6 μ g Se L⁻¹ and showed no spatial trend along the river (Table S1 in SI). All surface water samples were below the USEPA 5 μ g Se L⁻¹ aquatic life water quality criterion (24). On 9/28/04 only one site had Se concentrations above the detection limit. On 6/7/05 seven sites had Se concentrations above the detection limit. On 8/12/05 four sites had Se concentrations above the detection limit. The spring sampling event (6/7/05) had the most consistent Se concentrations above 1 μ g L⁻¹, a level at which some research predicts significant aquatic food chain bioaccumulation (25). Every waypoint along the BFR, except WP01 located at the mouth of the river, had Se concentrations above 1 μ g Se L⁻¹ during at least one sampling event. The pH of all BFR samples ranged from 7.8 to 8.6.

Total Se concentrations in BFR sediments ranged from less than 0.75 μ g Se g⁻¹ (method detection limit) to 5.5 μ g Se g⁻¹ (Table S2 in SI). There were no apparent trends in sediment Se concentration as a function of depth, sampling date, or location along the river, although waypoints 01, 02, 10, and 11 (near headwaters and the reservoir (Figure S1)) generally had lower sediment Se. Sediment Se levels were above 2.5 μ g g⁻¹, the suggested *predicted* effect level for fish and wildlife toxicity (26), at waypoints 03, 04, 06, and 08 on all sampling events (waypoint 08 was not sampled on the 6/7/05 sampling event). Sediment Se was above 4 μ g g⁻¹, the suggested *observed* effect level for fish and wildlife toxicity (26), at WP 03 and 04 during the September 2004 and August 2005 sampling events. Discussion of additional physico-chemical sediment properties is included in SI.

Sequential Extractions. Duplicate extractions were within 1–7% of each other. The difference between the total Se recovered from the pooled sequential extraction steps and the total Se measured independently was 2–61% of the total, with an average of 35% ($n = 10$). A second experiment on a smaller scale, designed to confirm or reject interpretations from the first sequential extraction experiment, reconciled the Se loss when Se concentrations in each extracted solution were above analytical detection limits, and confirmed all interpretations of Se species distributions from the first set of extractions (details in SI). Incomplete recovery is a known challenge when analyzing natural samples with low Se concentrations (27).

In the sampled BFR sediments, there was little difference in operationally defined Se speciation with depth, except at WP 10 in the delta of the Blackfoot Reservoir, which had 7% total extractable Se in the surficial sediment and 43% extractable Se at 19–21 cm (Figure 1). High-energy lotic systems are expected to have higher annual sediment turnover than slower moving systems, and thus the sediment profiles are expected to have more homogeneous physical and chemical profiles. There is variation in the Se speciation between the different samples (Figure 1). In summary, waypoints 01, 04, and 11 had 34–76% total extractable Se. Samples from WP 09 and 10A only had 7–11% total extractable Se.

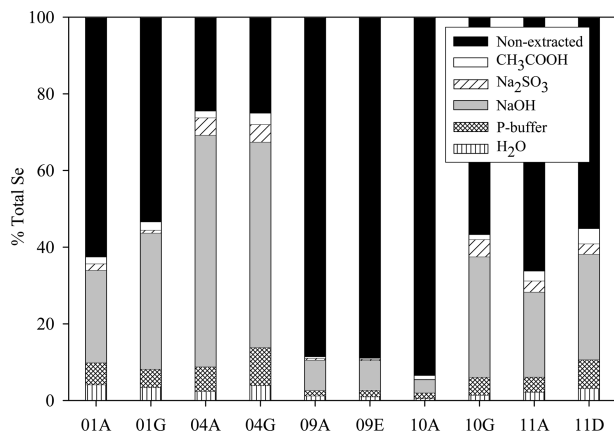


FIGURE 1. Percent of total Se extracted with each extracting solution for two depths of five waypoints along the Blackfoot River. Percentages are an average of duplicates. Total Se is calculated as the sum of extracted and nonextracted Se.

Water-soluble and ligand-exchangeable Se(VI) and Se(IV) are the most bioavailable fractions of Se (28). Phosphate can displace adsorbed Se into solution (29, 30). Soluble Se(-II) from proteins such as selenomethionine may also be extracted in these first steps (10, 28, 29). In all samples, a small percentage (less than 10%) of the total Se was extracted with water or P-buffer. Waypoint 04G had the highest (14%) and WP 10A had the lowest (2%) content of water-soluble Se plus ligand-exchangeable Se. The low percentage of soluble Se extracted (H₂O + P-buffer) is in agreement with the expected sediment speciation because oxyanions are highly soluble, and thus will likely be lost by mass transfer and diffusion into the above water column.

The NaOH extraction is designed to liberate Se associated with base-soluble soil organic matter (SOM), such as humic and fulvic acids, and Se(IV) tightly adsorbed to minerals or organic matter. Fifty-two to 80% of the total extracted Se was extracted with NaOH. Fifty to 60% of total Se from WP 04 (Figure 1), 25–35% from WP 01, 20–30% from WP 11, 30% from sample 10G, and less than 10% from the remaining samples was extracted with NaOH. This extraction step is highly selective for organically associated Se (10, 11, 28). The organically associated Se can exist as organic selenide compounds or Se(IV) strongly adsorbed onto organic-rich matrices, which is unable to be released by the preceding two extraction steps (10, 11, 28).

The sulfite extraction is efficient at solubilizing Se(0) because Se(0) and sulfite will form a soluble selenosulfate complex (11), and no significant overlap of selenide minerals or organic Se occurs (31). The primary source of Se(0) in sediments is reduction of oxyanions by bacteria and fungi (29), although in this lotic system physical translocation of host rock suspension may strongly contribute to the Se(0) fraction. The percentage of total Se extracted by sodium sulfite was minimal for all samples: 0.1–5% of the total Se (Figure 1). Therefore, biological reduction of Se(IV) or Se(VI) to stable Se(0) is expected to be minimal in BFR sediments.

Acetic acid is efficient at dissolving selenate ions isomorphically substituted for carbonate ions in minerals (10). The relative percentage of Se extracted by acetic acid in BFR sediments ranged from 0.3 to 4% of the total Se (Figure 1). Thus, Se substituted in the carbonate mineral lattice is minimal in BFR sediments.

In all samples except those from WP 04, the largest fraction of Se was nonextractable (53–93% nonextractable Se). Nonextractable Se can be selenide in either recalcitrant organic compounds or in minerals. XANES data and *ab initio* fitting of micro-EXAFS data from Ryser et al. (3) showed that the Se in the middle waste shale, the initial source of Se to

the BFR watershed, exists as both metal selenide minerals and diselenide carbon compounds. In addition, others have observed metal selenides in the mine-waste rock (4). These observed, nonextractable Se phases could be deposited into the BFR by meteoric erosion and downstream sedimentation. Kulp and Pratt (10) extracted Se from organic-rich shales in South Dakota and Wyoming and observed that nonextractable Se accounted for 20–62% of the total Se, and after an additional reduction step to reduce mineral selenides to hydrogen selenide, concluded that the majority of the nonextractable Se from shales was kerogen-bound organic Se complexes. The nonextractable Se from the BFR may also be bound in recalcitrant organic materials. Using transmission electron microscopy, X-ray diffraction, and infrared spectroscopy, Wen et al. (32) observed two types of Se in kerogen: embedded nanograins of elemental selenium and organically bound Se. In addition to settling of insoluble Se particles, sequestration of dissolved Se oxyanions into less mobile phases via biotic or abiotic pathways may be a source of this insoluble fraction. The full redox cycle of Se speciation observed in nature may be controlled by microorganisms (33), and studies have shown that several species of bacteria have the ability to reduce selenate, selenite, and elemental Se (34–39). In mine-affected WPRA soils, microbial populations have been isolated that reduce selenate to elemental Se (40).

Nonextractable Se can become soluble and mobile through oxidative weathering. Oxidation of Se in slurries and soils may occur under oxidizing aqueous environments or may be facilitated by microorganisms (33, 41, 42). Furthermore, oxidizing conditions are needed to degrade kerogen and release organically bound Se as a bioavailable ion (32). Kulp and Pratt (10) concluded that during oxidative weathering of Se-enriched shales, sedimentary organic matter (e.g., kerogen) appears to be converted to base-soluble humic substances. Biological and other influences on the degradation of recalcitrant, complex organic materials are unknown. Although selenide minerals and Se-substituted pyrite are relatively insoluble in reducing environments, the oxidation and dissolution of pyrite is an important process in natural waters (43). For example, arsenic in arsenopyrite can be released by oxidation at circumneutral pH (44). Therefore, dissolution of Se-substituted pyrite in BFR sediments may be a continuous, long-term source of dissolved Se into the water column. However, measured Se levels suggest the chemical flux of this process in higher-flow (June) and lower-flow (September) regimes is low enough to sustain overall water Se below 1.6 $\mu\text{g L}^{-1}$, which is lower than the current water quality criterion of 5 $\mu\text{g L}^{-1}$.

Selective extractions show that most Se in the BFR sediments is present as either (1) nonextractable Se (diselenide minerals or Se associated with recalcitrant organic matter), or (2) NaOH extractable Se (tightly sorbed Se(IV) or Se associated with base-soluble organic matter).

X-ray Spectroscopy. Sutton et al. (18) and Pickering et al. (19) achieved better signal deconvolution than possible in this study because the species in their samples were limited and known (i.e., the samples were spiked). In contrast our samples were collected from contaminated environments that have several possible Se species, are much lower in total Se concentration, and are highly susceptible to radiation damage with extensive exposure to the X-ray beam. The signal deconvolution algorithm used in this study is precise and accurate for categorizing Se into reduced Se (selenides and elemental Se), Se(IV), and Se(VI) oxidation states (additional details in SI, including Figures S2–S9).

Oxidation state maps were collected on a 2880 $\mu\text{m} \times 2000 \mu\text{m}$ area (144 \times 100 pixels), totaling 14,400 pixels of data for each sample (Figures S2, S4, S6, and S8 in SI). Oxidation state maps of Se(-II,0), Se(IV), and Se(VI) from a selected region

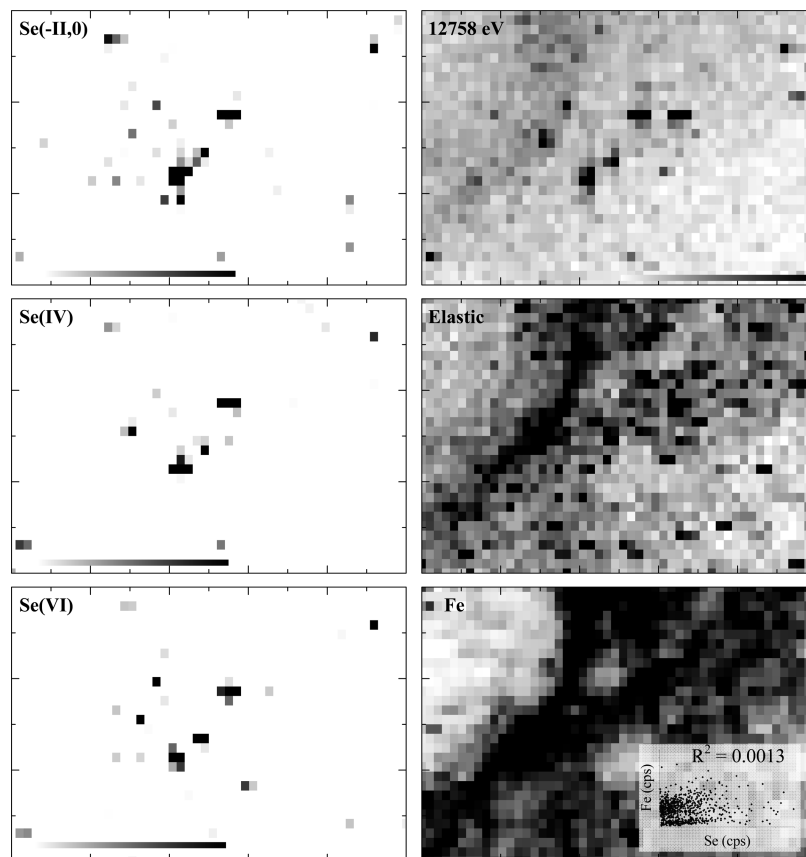


FIGURE 2. Micro-SXRF maps of a $1000 \times 600 \mu\text{m}$ region of interest from sample 09C. Each pixel shows deconvoluted signal. Se(-II,0) (12659 eV), Se(IV) (12663.5 eV), Se(VI) (12668.5 eV), total Se (12758 eV), elastic scattering, and total Fe fluorescence signals are shown. White to black gradient shows low to high intensity signal. An inset in Fe graph shows Fe v. Se correlation.

of the entire sample 09C map (Figure S8) are presented in Figure 2. There is a clear difference in pixel Se intensities at the three different energies. For instance, there are multiple Se hotspots that are visible on only one or two of the three oxidation state maps. The pixel intensity represents the relative amount of a specific Se valence. The total Se distribution is shown in the 12758.0 eV fluorescence map. The elastic scattering and Fe maps show the distribution of sediment particles and Fe, respectively.

From the energy specific maps, the fraction of each defined Se species for each pixel can be derived. Normalized ternary plots (Figure 3) show the fraction of each Se species at each pixel from each of the four samples. Se hotspots with signal from at least one Se species above background levels are plotted. In the four samples, the number of pixels with Se counts above background ranged between 338 and 779. Data at or near the apexes of the triangle indicate pixels that contain one Se oxidation state. Overlapping points are slightly offset to show that multiple points are present (e.g., Se(IV) apex on sample 04A diagram). To calculate the average percent Se species distribution, negative values were assigned a value of 0. The average fraction of total signal attributed to each Se oxidation state category was calculated (e.g., $X_1/(X_1 + X_2 + X_3)$) for each energy of each pixel, and the mean and standard error for these percentages were calculated for all Se hotspots in a sample (Table S3 in SI).

For sample 04A, the majority of the Se hotspots (415 of the 14400 pixels probed) were predominantly Se(IV), which is indicated by both oxidation state maps (Figure S2 in SI) and the ternary diagram (Figure 3). There were a significant number of data points that contained only Se(IV) or Se(VI). Within some $7 \mu\text{m} \times 7 \mu\text{m}$ spots, all three oxidation states were present, suggesting that different Se species may be associated with the same sediment particle. On average, the

Se hotspot pixels are 32% (± 1.3) Se(-II,0), 42% (± 1.4) Se(IV), and 26% (± 1.4) Se(VI). Applying a two-sample *t* test, the means are significantly different (p -value < 0.01). Thus, the percent of Se(IV) is significantly higher than the percent of both Se(-II,0) and Se(VI). Se(IV) dominated the pixel speciation distribution in sample 04A.

For sample 04G, the Se intensity in 338 of 14400 pixels was above background level (Figure S4 in SI). Similar to sample 04A, the species distributions at most of the pixels were combinations of two or more Se oxidation states (Figure 3). On average, the Se hotspot pixels are 30% (± 1.6) Se(-II,0), 44% (± 2.0) Se(IV), and 25% (± 1.8) Se(VI). The means are significantly different (p -value < 0.01), and the percent of Se(IV) is significantly higher than the percent of both Se(-II,0) and Se(VI). Speciation results from this bottom section are similar to the top 1–3 cm of the sample, 04A, although 04A shows more pixels with multiple Se species than 04G. This difference may be attributed to more variable redox processes in the surface sediment section.

The extraction analysis showed that 60% of the total Se in sample 04A and 54% of the total Se in sample 04G was extracted with NaOH, designed to liberate Se associated with base-soluble SOM and Se(IV) tightly adsorbed to either minerals or organic matter. Nine percent in sample 04A and 14% in sample 04G were soluble or exchangeable, and 25% in both samples was insoluble reduced species. The extraction results are consistent with the μ -SXRF results, which indicate that all three species were present, but Se(IV) predominated these samples.

The ternary plot of Se species from sample 09A (Figure 3) shows the fractionation of the Se oxidation state categories for 779 hotspot pixels. There is a clear predominance of pixels near the Se(-II,0) apex, indicating greater than 50% Se(-II,0). On average, the Se hotspots are 58% (± 1.0) Se(-II,0), 26%

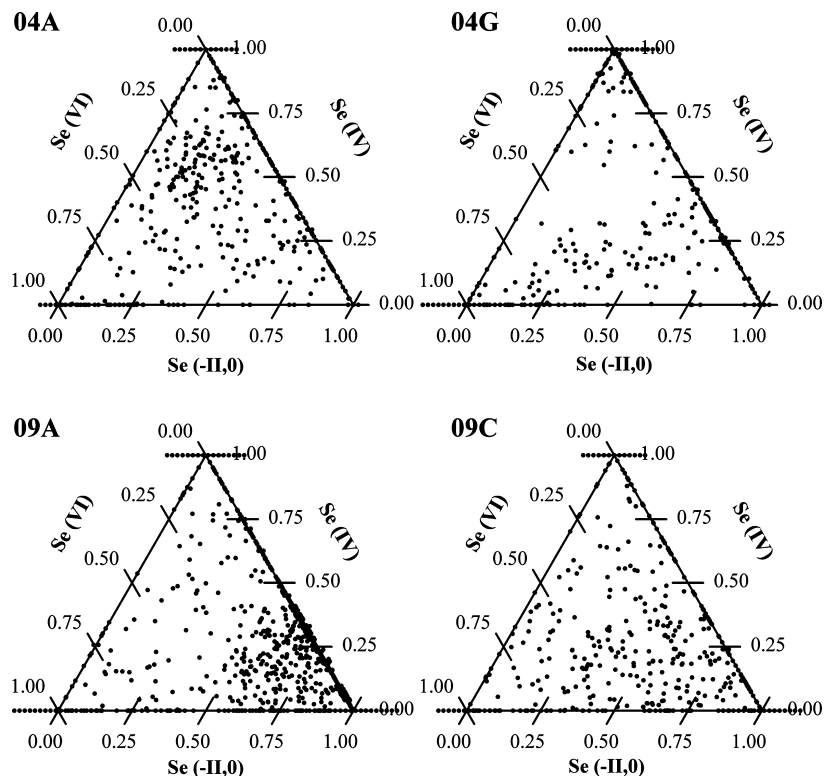


FIGURE 3. Ternary diagrams of Se valence distribution, derived from μ -SXRF data, of Se hotspots (above background levels) from four samples. Overlapping points are offset.

(± 0.90) Se(IV), and 16% (± 0.91) Se(VI). Sample 09C data are more concentrated on the axes, where pixels are composed of mixtures of either Se(-II,0) and Se(IV) or Se(-II,0) and Se(VI). On average, the Se hotspots in sample 09C (405 pixels) are 45% (± 1.5) Se(-II,0), 26% (± 1.4) Se(IV), and 29% (± 1.4) Se(VI). Many Se hotspots are a mixture of oxidation states, and all three defined oxidation states are present in both 09A and 09C. The mean distributions of each Se oxidation state category are significantly different (p -value < 0.01), and the percent of Se(-II,0) is significantly higher than the percent of both Se(IV) and Se(VI). Se(-II,0) is the predominant species in both WP 09 samples.

The extraction analysis revealed that 89% of the total Se in both WP 09 samples was not extracted and is either metal selenides or is associated with recalcitrant organic matter. Furthermore, only 8% was extracted with NaOH, which is Se associated with base soluble organic matter or tightly sorbed Se(IV), and only 3% was soluble or ion exchangeable. The extraction results are consistent with μ -SXRF results, which indicated Se(-II,0) species predominated.

The μ -SXRF data also allow the distinction between metal selenides and organic selenides, and between mineral-bound and organic-bound Se(IV). Selenium in each of the sediment samples was not spatially associated with Fe, Zn, Cu, Ca, or other elements of interest. For example, the Pearson correlation coefficients for Se intensity versus Fe intensity for Se hotspots for samples 04A, 04G, 09A, and 09C are 0.136, -0.192, 0.151, and 0.0829, respectively. Even when regions of interest from the larger maps were isolated, there were no correlations (e.g., inset in Figure 2 Fe distribution map). Furthermore, no correlations were observed between Fe and Se distribution maps (Figure 2). The lack of correlations of Se with metals (Fe, Cu, and Zn) suggests that neither metal selenides nor Se(IV) associated with oxides are likely BFR sediment species. Significant correlations between Fe and Se have been observed in soils and host-rock material from the WPRA (3, 17). The lack of metal selenides or elemental Se in the sediments suggests that these phases, which were

present in the shale, have dissolved, and the recalcitrant organo-selenides in the samples (particularly WP09) likely persist from the eroded shale. In samples from WP 04, the lack of Se(IV) correlation with metals confirms that Se is tightly bound to organic matter sediment fractions. The molecular structure of the Se(IV)-organic compounds remains unclear. If the structure was Se adsorbed onto organic functional groups, then the phosphate extraction step should release most of the bound Se by ligand exchange.

Coupling both macroscale and molecular-level information, we conclude that Se in Blackfoot River sediments is likely present as (1) Se(-II) associated with recalcitrant organic matter, and (2) Se(IV) tightly bound to organic materials. Other research relying on macroscale techniques has suggested that the majority of Se in pond and stream sediments is associated with organic carbon (13, 26, 28). In-situ Se speciation data on BFR sediment samples confirms that Se-organic matter associations are important phases in sediment environments; however, the biogeochemical cycling of sedimentary organic matter is not well understood.

Selenium speciation in sediments depends on multiple interacting biological, chemical, and physical processes that can release or sequester Se in sediment environments, making predictions of Se mobility highly complex (25, 42, 45, 46). Moreover, direct uptake of Se by plants, insects, bottom-dwelling organisms, and detritus-feeding fish and wildlife are important pathways that can affect the dynamics of Se biogeochemical cycling in sediments (45, 47). Differences between sediment Se species (i.e., WP 04 and WP 09 samples) are attributed to these complex sediment processes that are likely variable across the stream sediments.

By knowing that tightly sorbed Se oxyanions and reduced Se associated with recalcitrant organic matter are the prevalent species of Se in BFR sediments, we can predict that BFR sediment Se is sequestered in immobile phases, and is only mobile after biological, physical, or chemical mobilization processes occur. Understanding the sediment Se speciation will help guide further experimentation to

determine reaction mechanisms that control the cycling of these species. Variables in these reactions can then be managed to minimize mobilization and bioavailability to prevent risks to ecosystems from Se-affected sediments.

Acknowledgments

Funding for this research was provided by the USEPA, grant ID X970339010. The Advanced Light Source, where much of this research was conducted, is supported by the Director, Office of Science, Office of Basic Energy Sciences, and the Materials Sciences Division of the U.S. Department of Energy under contract DE-AC03-76SF00098 at the Lawrence Berkeley National Laboratory. Assistance on this project was graciously provided by Drs. Brian Hart and Leslie Baker at the University of Idaho.

Supporting Information Available

Further discussion of methods, X-ray signal deconvolution, and results are included. Additional figures and tables include a map of the sampling sites; total water Se and sediment Se tables; oxidation state maps of samples 04A, 04G, 09A, and 09C; transect data showing signals before and after signal deconvolution; and a table with the average Se species composition for each sample.

Literature Cited

- Mislevy, P.; Blue, W. G.; Stricker, J. A.; Cook, B. C.; Vice, M. J. Phosphate mining and reclamation In *Reclamation of Drastically Disturbed Lands*; Barnhisel, R. I., Darmody, R. G., Daniels, W. L., Eds.; American Society of Agronomy: Madison, WI, 2000; Vol. 41, pp 961–1005.
- Munkers, J. P. Abiotic and biotic processes in the release and control of selenium in the Western Phosphate Resource Area. Environmental Science, University of Idaho: Moscow, ID, 2000; p 123.
- Ryser, A. L.; Strawn, D. G.; Marcus, M. A.; Johnson-Maynard, J. L.; Gunter, M. E.; Möller, G. Micro-spectroscopic investigation of selenium-bearing minerals from the Western US Phosphate Resource Area. *Geochem. T.* **2005**, *6*, 1–11.
- Perkins, R. B.; Foster, A. L. Mineral affinities and distribution of selenium and other trace elements in black shale and phosphorite of the Phosphoria formation In *Life Cycle of the Phosphoria Formation: From Deposition to Post-Mining Environment*; Hein, J. R., Ed.; Elsevier B. V.: Amsterdam, Netherlands, 2004; Vol. 8, pp 251–295.
- Hamilton, S. J.; Buhl, K. J. Selenium in water, sediment, plants, invertebrates, and fish in the Blackfoot River drainage. *Water, Air, Soil Pollut.* **2004**, *159*, 3–34.
- Piper, D. A.; Skorupa, J. P.; Presser, T. S.; Hardy, M. A.; Hamilton, S. J.; Huebner, M.; Gulbrandsen, R. A. *The Phosphoria Formation at the Hot Springs Mine in Southeastern Idaho: a Source of Selenium and Other Trace Elements to Surface Water, Ground Water, Vegetation, and Biota*; United States Geological Survey Open File Report 00-050; USGS, 2000.
- Fessler, A. J.; Möller, G.; Talcott, P.; Exon, J. Selenium toxicity in sheep grazing reclaimed phosphate mining sites. *Vet. Hum. Toxicol.* **2003**, *45*, 294–298.
- Cutter, G. A. Determination of selenium speciation in biogenic particles and sediments. *Anal. Chem.* **1985**, *57*, 2951–2955.
- Sappington, K. G. Development of aquatic life criteria for selenium: a regulatory perspective on critical issues and research needs. *Aquat. Toxicol.* **2002**, *57*, 101–113.
- Kulp, T. R.; Pratt, L. M. Speciation and weathering of selenium in Upper Cretaceous chalk and shale from South Dakota and Wyoming, USA. *Geochim. Cosmochim. Acta* **2004**, *68*, 3687–3701.
- Wright, M. T.; Parker, D. R.; Amrhein, C. Critical evaluation of the ability of sequential extraction procedures to quantify discrete forms of selenium in sediments and soils. *Environ. Sci. Technol.* **2003**, *37*, 4709–4716.
- Zhang, Y.; Moore, J. N.; Frankenberger, W. T. Speciation of soluble selenium in agricultural drainage waters and aqueous soil-sediment extracts using hydride generation atomic absorption spectrometry. *Environ. Sci. Technol.* **1999**, *33*, 1652–1656.
- Martens, D. A.; Suarez, D. L. Selenium speciation of soil/sediment determined with sequential extractions and hydride generation atomic absorption spectrophotometry. *Environ. Sci. Technol.* **1997**, *31*, 133–139.
- Tokunaga, T. K.; Sutton, S. R.; Bajt, S.; Nuessle, P.; Shea-McCarthy, G. Selenium diffusion and reduction at the water-sediment boundary: Micro-XANES spectroscopy of reactive transport. *Environ. Sci. Technol.* **1998**, *32*, 1092–1098.
- Ryser, A. L. Biogeochemistry of Selenium in Reclaimed Mine Soils of the Western Phosphate Resource Area. In *Plant, Soil, and Entomological Sciences*; University of Idaho: Moscow, ID, 2005; p 154.
- Smith, P.; Koch, I.; Gordon, R.; Mandoli, D.; Chapman, B.; Reimer, K. X-ray absorption near-edge structure analysis of arsenic species for application to biological environmental samples. *Environ. Sci. Technol.* **2005**, *39*, 248–254.
- Ryser, A. L.; Strawn, D. G.; Marcus, M. A.; Fakra, S.; Johnson-Maynard, J. L.; Möller, G. Microscopically focused synchrotron X-ray investigation of selenium speciation in soils developing on reclaimed mine lands. *Environ. Sci. Technol.* **2006**, *40*, 462–467.
- Sutton, S. R.; Bajt, S.; Delaney, J.; Schulze, D.; Tokunaga, T. K. Synchrotron x-ray fluorescence microprobe: quantification and mapping of mixed valence state samples using micro-XANES. *Rev. Sci. Instrum.* **1995**, *66*, 1464–1467.
- Pickering, I. J.; Prince, R. C.; Salt, D. E.; George, G. N. Quantitative, chemically specific imaging of selenium transformation in plants. *Proc. Natl. Acad. Sci. U. S. A.* **2000**, *97*, 10717–10722.
- Hamilton, S. J.; Lemly, A. D. Water-sediment controversy in setting environmental standards for selenium. *Ecotoxicol. Environ. Safe.* **1999**, *44*, 227–235.
- Lemly, A. D. *Selenium Assessment in Aquatic Ecosystems: A Guide for Hazard Evaluation and Water Quality Criteria*; Springer-Verlag Publishers: New York, 2002.
- Canton, S. P.; Van Derveer, W. D. Selenium toxicity to aquatic life: an argument for sediment-based water quality criteria. *Environ. Toxicol. Chem.* **1997**, *16*, 1255–1259.
- Marcus, M. A.; MacDowell, A. A.; Celestre, R.; Manceau, A.; Miller, T.; Padmore, H. A.; Sublett, R. E. Beamline 10.3.2 at ALS: a hard X-ray microprobe for environmental and materials science. *J. Synchrotron Radiat.* **2004**, *11*, 239–247.
- USEPA. *Draft selenium aquatic life criterion*; <http://www.epa.gov/seleniumcriteria/>; 2004.
- Peters, G. M.; Maher, W. A.; Barford, J. P.; Gomes, V. G. Selenium associations in estuarine sediments: redox effects. *Water, Air, Soil Pollut.* **1997**, *99*, 275–282.
- Van Derveer, W. D.; Canton, S. P. Selenium sediment toxicity thresholds and derivation of water quality criteria for freshwater biota of western streams. *Environ. Toxicol. Chem.* **1997**, *16*, 1260–1268.
- Zhang, Y.; Liu, G.; Chou, C.-L.; Wang, L.; Kang, Y. Sequential solvent extraction for the modes of occurrence of selenium in coals of different ranks from the Huaiabei Coalfield, China. *Geochem. J.* **2007**, *8*.
- Martens, D. A.; Suarez, D. L. Selenium speciation of marine shales, alluvial soils, and evaporation basin soils of California. *J. Environ. Qual.* **1997**, *26*, 424–432.
- Ponce de Leon, C.; DeNicola, K.; Montes Bayon, M.; Caruso, J. A. Sequential extractions of selenium soils from Stewart Lake: total selenium and speciation measurements with ICP-MS detection. *J. Environ. Monit.* **2003**, *5*, 435–440.
- Dhillon, S. K.; Dhillon, K. S. Selenium adsorption in soils as influenced by different anions. *J. Plant Nutr. Soil Sci.* **2000**, *163*, 577–582.
- Velinsky, D. J.; Cutter, G. A. Determination of elemental selenium and pyrite-selenium in sediments. *Anal. Chim. Acta* **1990**, *235*, 419–425.
- Wen, H.; Carignan, J.; Qiu, Y.; Liu, S. Selenium speciation in kerogen from two Chinese selenium deposits: environmental implications. *Environ. Sci. Technol.* **2006**, *40*, 1126–1132.
- Dowdle, P. R.; Oremland, R. S. Microbial oxidation of elemental selenium in soil slurries and bacterial cultures. *Environ. Sci. Technol.* **1998**, *32*, 3749–3755.
- Oremland, R. S.; Hollibaugh, J. T.; Maest, A. S.; Presser, T. S.; Miller, L. G.; Culbertson, C. W. Selenate reduction to elemental selenium by anaerobic bacteria in sediments and culture; biogeochemical significance of a novel, sulfate-independent respiration. *Appl. Environ. Microbiol.* **1989**, *55*, 2333–2343.

- (35) Oremland, R. S.; Blum, J. S.; Bindi, A. B.; Dowdle, P. R.; Herbel, M.; Stolz, J. F. Simultaneous reduction of nitrate and selenate by cell suspensions of selenium-respiring bacteria. *Appl. Environ. Microbiol.* **1999**, *65*, 4385–4392.
- (36) Kenward, P. A.; Fowle, D. A.; Yee, N. Microbial selenate sorption and reduction in nutrient limited systems. *Environ. Sci. Technol.* **2006**, *40*, 3782–3786.
- (37) Doran, J. W. Microorganisms and the biological cycling of selenium. In *Advances in Microbial Ecology*; Marshall, K. C., Ed.; Plenum Press: New York, 1982; pp 1–32.
- (38) Fujita, M.; Ike, M.; Kashiwa, M.; Hashimoto, R. Laboratory-scale continuous reactor for soluble selenium removal using selenate-reducing bacterium, *Bacillus* sp. SF-1. *Biotechnol. Bioeng.* **2002**, *80*, 755–761.
- (39) Herbel, M.; Blum, J. S.; Borglin, S. E.; Oremland, R. S. Reduction of elemental selenium to selenide: experiments with anoxic sediments and bacteria that respire Se-oxyanions. *Geomicrobiology* **2003**, *20*, 587–602.
- (40) Knotek-Smith, H.; Crawford, D.; Möller, G.; Henson, R. Microbial studies of a selenium-contaminated mine site and potential for on-site remediation. *J. Ind. Microbiol. Biot.* **2006**, *33*, 897–913.
- (41) Losi, M. E.; Frankenberger, W. T. Microbial oxidation and solubilization of precipitated elemental selenium in soil. *J. Environ. Qual.* **1998**, *27*, 836–843.
- (42) Masscheleyn, P. H.; Delaune, R. D.; Patrick, J.; William, H. Transformations of selenium as affected by sediment oxidation-reduction potential and pH. *Environ. Sci. Technol.* **1990**, *24*, 91–96.
- (43) Singer, P. C.; Stumm, W. Acidic mine drainage: the rate-determining step. *Science* **1970**, *167*, 1121–1123.
- (44) Walker, F. P.; Schreiber, M. E.; Rimstidt, D. J. Kinetics of arsenopyrite oxidative dissolution by oxygen. *Geochim. Cosmochim. Acta* **2006**, *70*, 1668–1676.
- (45) Lemly, A. D. Selenium transport and bioaccumulation in aquatic ecosystems: a proposal for water quality criteria based on hydrological units. *Ecotoxicol. Environ. Safe.* **1999**, *42*, 150–156.
- (46) Stillings, L. L.; Amacher, M. C. Selenium attenuation in a wetland formed from mine drainage in the Phosphoria Formation, Southeast Idaho In *Life Cycle of the Phosphoria Formation: From Deposition to Post-Mining Environment*; Hein, J. R., Ed.; Elsevier B. V.: Amsterdam, Netherlands, 2004; Vol 8, pp 467–482.
- (47) Andrahennadi, R.; Wayland, M.; Pickering, I. J. Speciation of selenium in stream insects using X-ray absorption spectroscopy. *Environ. Sci. Technol.* **2007**, *41*, 7683–7687.

ES7032229